Check for
updates

Improvement of the performance parameters of the surface plasmon resonance biosensor using Al_2O_3 and WS_2

Jannati Nabiha Nur[1] · Mohammad Hasibul Hasan Hasib[1] [ORCID] **· Fairuj Asrafy[1] · Kamrun Nahar Shushama[1] · Reefat Inum[1] · Md. Masud Rana[1]**

Abstract

Here, proposed Kretschmann configuration based surface plasmon resonance biosensor shows immense improvement in its performance parameters. This highly sensitive biosensor provides a higher value of quality factor and detection accuracy. We presented a five-layer model of a biosensor with two dimensional transition metal di-chalcogenides Tungsten disulfide (WS2) in addition with Al2O3 layer. By using one layer of WS2 with six layers of Al2O3, the highest sensitivity (227.5 °/RIU), detection accuracy (1.1123), and quality factor (28.26 RIU^{-1}) can be achieved. CaF2 as coupling prism has also played a remarkable role in enhancing the performance parameters for its low refractive index.

1 Introduction

An optical sensor is a sensing device which determines the desired quantity by measuring the change in refractive index, absorbance and fluorescence properties of analyte molecules (Wolfbeis 1991; Boisdé and Alan 1996). For the purpose of chemical and biomedical sensing, various optical methods like ellipsometry (Wang et al. 2003), spectroscopy (Rowe-Taitt et al. 2000), interferometry (Heideman et al. 1993) and surface plasmon resonance (SPR) (Homola 2003) have been used.

SPR is a widely preferred surface sensitive optical analysis technique which is capable of determining the properties of ultrathin films when full angular spectra are measured (Albers and Vikholm-Lundin 2011). SPR sensor can be classified on the basis of angular shift, wavelength, intensity, phase or polarization modulation (Homola and Marek 2006). In SPR sensors with angular modulation, surface plasmon (SP) is generated by the interaction between the incident transverse magnetic (TM) polarized light and the free electron in the metal surface. SP is actually the electronic density wave that propagates along the

---

✉ Mohammad Hasibul Hasan Hasib
   hasib.eee.ruet@gmail.com

[1] Department of Electrical and Electronic Engineering, Rajshahi University of Engineering & Technology, Rajshahi, Bangladesh

metal surface. The incident light resonantly couples with SP when the vector of an incident light matches with the wave vector of a surface plasmon wave (SPW). After that incident, an enormous electric-field can be observed which is referred to as surface plasmon resonance (SPR). Multiple angles of incidence of the light wave can be observed owing to the fluctuation of the strength of coupling between the incident wave and the SP. The angle of incidence because of the strongest coupling is measured and used as the sensor output. Refractive index of the sensing medium can be used to calibrate the sensor (Otto 1968; Kretschmann and Raether 1968; Matsubara et al. 1988). SPR based biosensor has gained huge popularity in the research field as it offers label-free and real-time detection technique for monitoring bio-molecular analysis. Application fields of SPR based biosensor are the detection of enzyme, environment, food safety (Homola 2003; Pumera 2011), antibody-antigen connection (Pei et al. 2000), DNA–DNA hybridization (Shushama et al. 2017) and so on. Due to having some limitations in Otto configuration, the modified SPR based on Kretschmann configuration is preferred (Kretschmann and Raether 1968). Al_2O_3 provides minimized loss in the performance of the biosensor because of its refractive index. Another property that contributes to the sensor improvement that is the uniformity of the Al_2O_3 layer (Sharma 2012).

The basic form of the Kretschmann configuration is a coupling prism and metal film. Silver, copper, aluminium, sodium and indium can be used as SPR active metal on the prism. Because of having the most practical nature with good resistance to oxidation and corrosion in different environment, stable and superior performance, gold is chosen over all other SPR materials (Shushama et al. 2017). Numerous technique based on particles in nanoscale can be utilized for the betterment of the sensor's performance (Zhao 2006; Stewart et al. 2008). As Au layers have a limitation in absorbing biomolecules, so sensing layers can be introduced to enhance the sensitivity (Verma et al. 2015; Biednov et al. 2015). Recently, plenty of research works have been carried out using various layers for improved performance of the biosensor. Sensitivity increases as more biomolecules are absorbed. Mishra et al. (2015) used Si layer over the conventional Kretschmann configuration for better sensitivity. Ouyang et al. (2016) demonstrated the use of TMDC material MoS_2 along with Si for further improvement in sensitivity, Rahman et al. (2018) showed the use of another TMDC material WS_2 for better sensitivity, quality factor and detection accuracy.

Further improvement in the performance parameters than previous works can be attainable. Here we proposed a five-layer Kretschmann configuration based SPR biosensor model consisting of Al_2O_3 and WS_2 layers and the number of layers are optimized in such a way to give out the best possible result.

2 Theoretical model and design consideration

Using five layers in the proposed model, SPR biosensor is analyzed. Figure 1 represents the configuration of the proposed biosensor. The excitation light of 633 nm wavelength is used for the SPR sensing. The TM-polarized light is incident on the one lateral side of the prism and reflected from another lateral side after reaching to the base. A photodetector is used to analyze that reflected light. Here, the proposed biosensor consists of Au layer, Al_2O_3 layer, transition metal di-chalcogenides WS_2 and sensing layer.

N-layer model is considered to obtain the expression for the reflected light. Transfer matrix method (TMM) and Fresnel equations based on that N-layer model are used to peruse the optical characteristics of multi-layers. The TMM is employed for a better
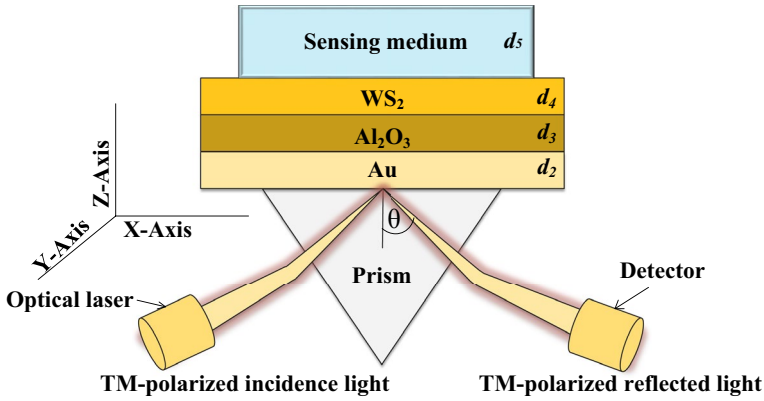
Fig. 1 Schematic of experimental realization of WS$_2$ and Al$_2$O$_3$ based SPR biosensor

understanding of the change in the reflectivity of SPR sensors. All layers are assumed to be stacked in parallel manner along the z-axis and the z-axis is considered to be perpendicular with the thickness d_k of these layers. Other common features of any layers are dielectric constant ε_k, permeability μ_k and refractive index n_k where suffix k represents the prism, Au metal, Al$_2$O$_3$, WS$_2$, sample or the sensing medium. It is taken into account that each and every layer is uniform, isotropic and non-magnetic in nature. The boundary conditions for theoretical modelling is denoted by Z. Here, $Z_1 = 0$ defines the tangential field of the first boundary and Z_{N-1} is considered for the last boundary (Zeng et al. 2015).

$$\begin{bmatrix} p_1 \\ Q_1 \end{bmatrix} = M \begin{bmatrix} P_{N-1} \\ Q_{N-1} \end{bmatrix} \tag{1}$$

where, P and Q are the tangential components of electrical and magnetic fields at the interface boundary of the layers. The characteristics matrix for the combined structure of the N-layer model of the sensor and for p-polarized light can be expressed by *M*.

$$M_{ij} = \left(\prod_{K=2}^{N-1} M_K \right) = \begin{bmatrix} M_{11} & M_{12} \\ M_{21} & M_{22} \end{bmatrix} \tag{2}$$

where K represents the Kth layer of the N-layered model (Wu et al. 2010).

Now M_k for the TMM waves of the incident light,

$$M_K = \begin{bmatrix} \cos \beta_K & (-i \sin \beta_K / q_K) \\ -i q_K \sin \beta_K & \cos \beta_K \end{bmatrix} \tag{3}$$

Here, q_k and β_K help to obtain the four elements M$_{11}$, M$_{12}$, M$_{21}$ and M$_{22}$ of the matrix M

$$q_K = \sqrt{\frac{\mu_K}{e_K}} \cos \theta_K = \frac{\sqrt{(e_K - n_1^2 \sin^2 \theta_1)}}{e_K} \tag{4}$$

and

$$\beta_K = \frac{2\pi d_K}{\lambda}\sqrt{(e_K - n_1^2 \sin^2 \theta_1)} \tag{5}$$

$\theta_1 =$ incident angle for the first layer.

Now the systematic complex reflection co-efficient (r_p) for the combined N-layered structure is calculated by means of TMM for P-polarized light.

$$r_p = \frac{(M_{11} + M_{12qN})q_1 - (M_{21} + M_{22qN})}{(M_{11} + M_{12qN})q_1 + (M_{21} + M_{22qN})} \tag{6}$$

The corresponding reflectivity R_p for defined multilayer configuration is given by

$$R_p = \left| r_p \right|^2 \tag{7}$$

3 Performance parameters of the SPR sensor

The main parameters on which the performance of the SPR biosensor depend are sensitivity, detection accuracy and the quality factor. For an efficient sensor, all these three parameters should be as high as possible (Pal et al. 2017). The sensitivity (S) is theoretically the ratio of the deviation in the resonance angle of incidence to the refractive index change of the sensing medium (Lin et al. 2016). The unit of the sensitivity is °/RIU.

$$S = \frac{\delta\theta}{\Delta n_s} \tag{8}$$

Detection accuracy (DA) is another important parameter which helps to determine the resolution of the SPR sensor. DA can be compared to the signal to noise ratio (SNR). The full width at a half maximum (FWHM) of the reflectance curve is necessary to calculate the DA. Low FWHM decreases the uncertainty in determination of the resonance dip and as a consequence, it increases the resolution of the sensor. Now, DA is actually the ratio of the deviation in resonance angle to the FWHM (Pal et al. 2017).

$$DA = \frac{\theta_{res}}{FWHM} \tag{9}$$

Lastly, the Quality factor (Q) is the ratio of the sensitivity to the FWHM of the reflectance curve. The unit of the Q is RIU^{-1} (Rahman et al. 2018)

$$Q = \frac{S}{FWHM} \tag{10}$$

The proposed five-layer model is composed of BK7 prism, Au, Al_2O_3, WS_2 and lastly the sensing medium.

3.1 Refractive index of various layers

In this proposed model BK7 prism is the first layer. Au film is the second layer with the thickness d_2. The third layer is Al_2O_3 and its thickness is denoted by d_3. WS_2 is the fourth layer with the thickness d_4. Each layer of WS_2 is 0.8 nm (Lin et al. 2016). Now the refractive index of BK7 prism is n_{BK7}.

$$n_{BK7} = \sqrt{\left(\frac{1.03961212\lambda^2}{\lambda^2 - 0.00600069867} + \frac{0.231792344\lambda^2}{\lambda^2 - 0.0200179144} + \frac{1.03961212\lambda^2}{\lambda^2 - 103.560653} + 1 \right)}$$

(11)

Here λ = Wavelength (μm) of the incident light = 633 nm.

According to Drude formula, the refractive index (n_m) of Au metal (Shushama et al. 2017).

$$n_m = \sqrt{\left[1 - \frac{\lambda^2 \lambda_C}{\lambda_P^2 (\lambda_C + i\lambda)} \right]}$$

(12)

where λ_P = plasma wavelength = 1.6826×10^{-7} m λ_C = collision wavelength = 8.9342×10^{-6} m

Refractive index of the Al_2O_3 at 633 nm of wavelength is 1.7659 and WS_2 is $4.89 + 0.314i$. Refractive index of the sensing medium is 1.33 (Ouyang et al. 2017).

4 Result and discussion

In this paper, four structures are considered to evaluate the improvement done in the proposed model. (a) Structure no. 1 (Au = 47 nm, Al_2O_3 = 0 nm, WS_2 = 0 nm), (b) Structure no. 2 (Au = 47 nm, Al_2O_3 = 6mn, WS_2 = 0 nm, (c) Structure no. 3 (Au = 47 nm, Al_2O_3 = 0 nm, WS_2 = 0.8 nm), (d) Structure no. 4 (Au = 47 nm, Al_2O_3 = 6 nm, WS_2 = 0.8 nm). The range of the refractive index is taken 1.335 to 1.375. Change in RI of the sensing medium is responsible for the molecular binding. dn/dc depicts the slope of the RI (n) change of the solution in accordance with the change in concentration (c) of that solution. For HPS concentration minus cmc ($cmc_{HPS} = 1 \times 10^{-4}$), it is shown that for 0.002 g/cm³ change in

Fig. 2 Sensitivity versus refractive index of four structures
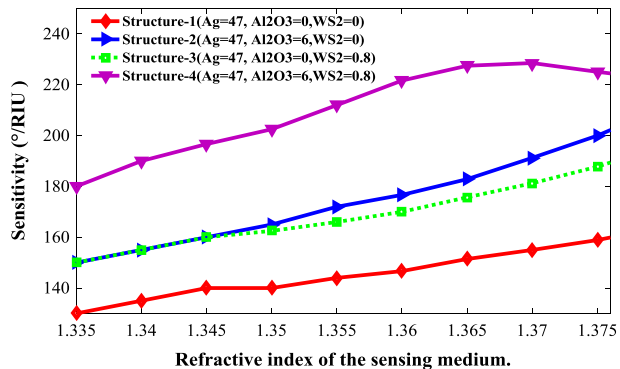
concentration, excellent linearity is shown when the range of RI is taken 1.335 to 1.3375 with 0.005 interval (Tumolo et al. 2004). This is the reason behind taking this specific range of RI from 1.335 to 1.375 in designing the proposed model.

Sensitivities for four classified structures have been plotted for the specified range of RI of the sensing medium in Fig. 2 It is seen that in structure no. 1 where Al_2O_3 and WS_2 layers are absent then sensitivity increases from 130 to 158.89°/RIU for the change in the RI of the sensing medium from 1.335 to 1.375. In structure no. 2, after adding Al_2O_3, sensitivity increases from 150 to 200°/RIU. Later on structure no. 3, WS_2 is added with the first structure keeping Al_2O_3 absent the obtained sensitivity range is 150–186.78°/RIU and it is comparatively lower than the structure 2. Finally, in the case of the proposed model presented by structure no. 4 where both Al_2O_3 and WS_2 are present, a significant increase in the sensitivity is observed. For the change in RI from 1.335 to 1.375, the sensitivity changes from 180 to 211.11°/RIU and the highest sensitivity 227.50°/RIU is obtained at 1.37. That is why 1.37 is chosen for further analysis where the resonance angle shift is determined from the reflectivity curve.

In Fig. 3 Reflectivity versus angle of incidence is plotted for four individual structures above mentioned. Angle shift is administered by RI values 1.33 and 1.37 both. So, four structures individually exhibit reflectivity curves for refractive indices 1.33 and 1.37 respectively. At the RI value of 1.33, the sensor surfaces the basic initial point before the sensing starts and at 1.37 it corroborates the maximum sensitivity. For all four cases, Δn has a constant value of 0.04. In Fig. 3a for first structure, $\Delta\theta = 6.2°$ and the sensitivity (S) is 155°/RIU at 1.37. For the second structure in Fig. 3b, when Δn is 0.04, we get $\Delta\theta = 7.65°$ and S = 191.25°/RIU. Figure 3c represents the third structure where $\Delta\theta = 7.25°$ and S = 181.25°/RIU. In Fig. 3d, for the fourth structure greatest angular shift (9.1°) is observed with the highest sensitivity (227.5°/RIU).
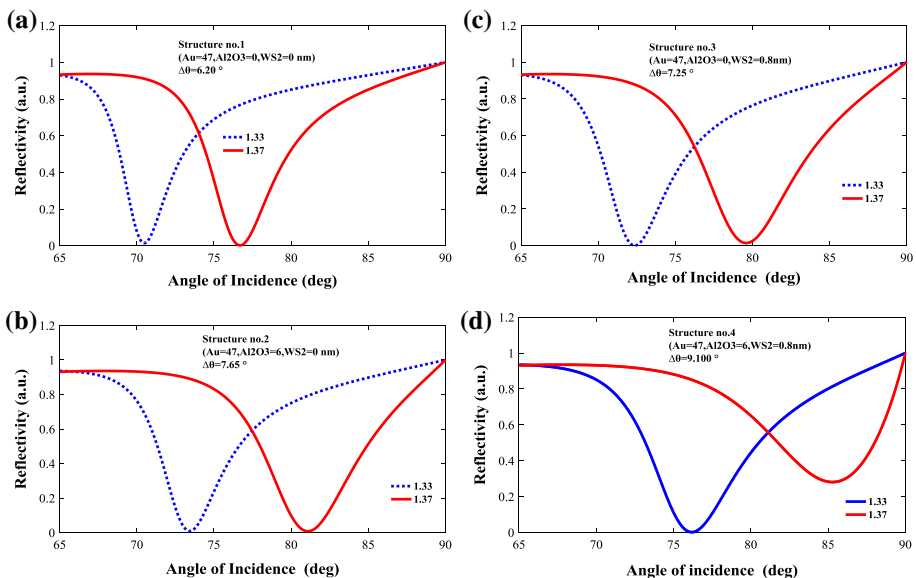

Fig. 3 Reflectivity versus angle of incidence **a** structure no. 1 **b** structure no. 2 **c** structure no. 3 **d** structure no. 4

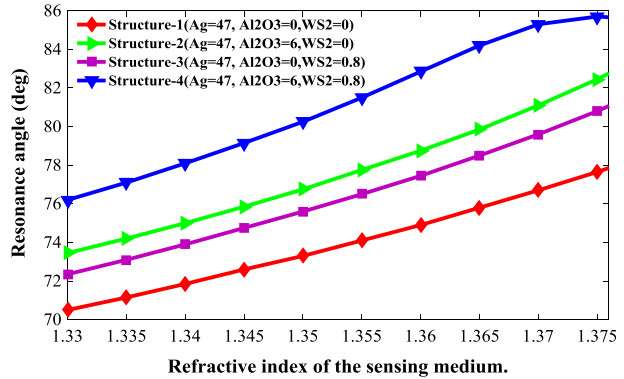**Fig. 4** Resonance angle versus refractive index for four structures

Table 1 Summarization of overall result for four structures

Structure	Configuration	$\delta\theta$	FWHM	Sensitivity (°/RIU)	DA	Q (RIU^{-1})
1	Au = 47 nm, Al$_2$O$_3$ = 0 nm, WS$_2$ = 0 nm	6.2	5	155	1.24	31
2	Au = 47 nm, Al$_2$O$_3$ = 6 nm, WS$_2$ = 0 nm	7.65	6.55	191.25	1.16	29.198
3	Au = 47 nm, Al$_2$O$_3$ = 0 nm, WS$_2$ = 0.8 nm	7.25	6.9	181.25	1.05	26.268
4	Au = 47 nm, Al$_2$O$_3$ = 6 nm, WS$_2$ = 0.8 nm	9.1	8.05	227.25	1.14	28.26

Because of the change in the RI of the sensing medium, the change in the resonance angle can be found which is denoted by θ_{res}. In Fig. 4 we have plotted the resonance angles versus the RI for previously mentioned four structures. The same RI range (1.33 to 1.375) is employed here. Highest resonance angle range from 76.20° to 85.5° is perceived for the structure no. 4. Maximum resonance angle 85.7° is manifested by 1.37. This outcome reinforces the reliability of the proposed model using Au, Al$_2$O$_3$, WS$_2$.

Table 1 summarizes the overall result obtained from all four structures. It is clearly shown that structure no. 4 gives the highest sensitivity of 227.5°/RIU. On the contrary, structure no. 1 gives the maximum value for quality factor and detection accuracy respectively 31 and 1.24 with the lowest sensitivity of 155°/RIU. As sensitivity is a very important parameter for a biosensor and lower sensitivity is not desirable, so the structure no. 4 is considered as the most optimized one.

Layers in this configuration are optimized very cautiously. For having the main focus on designing a highly sensitive SPR biosensor, sensitivity has been the most prominent factor to be considered while optimizing.

In Fig. 5a the width of Au layer is optimized and the maximum sensitivity 227.5°/RIU is discerned at 47 nm. The optimization of Au layer has been simulated for a width range from 40 to 65 nm.Sensitivity gradually increases up to 47 nm but afterwards it decreases which underlies the rationalization of elected width of Au layer at 47 nm. Figure 5b illustrates the change in sensitivity by changing the thickness of WS$_2$ layer. It attributes that valid positive sensitivity can be acquired by only monolayer or bilayer WS$_2$ and so Fig. 5c reveals the reflectivity curve for these two valid cases. Monolayer of WS$_2$ is scored for giving highest the sensitivity with thickness of 0.8 nm. In Fig. 5d it is realized that at six layers of Al$_2$O$_3$ highest sensitivity can be achieved. Figure 5e exposes how reflectivity curves
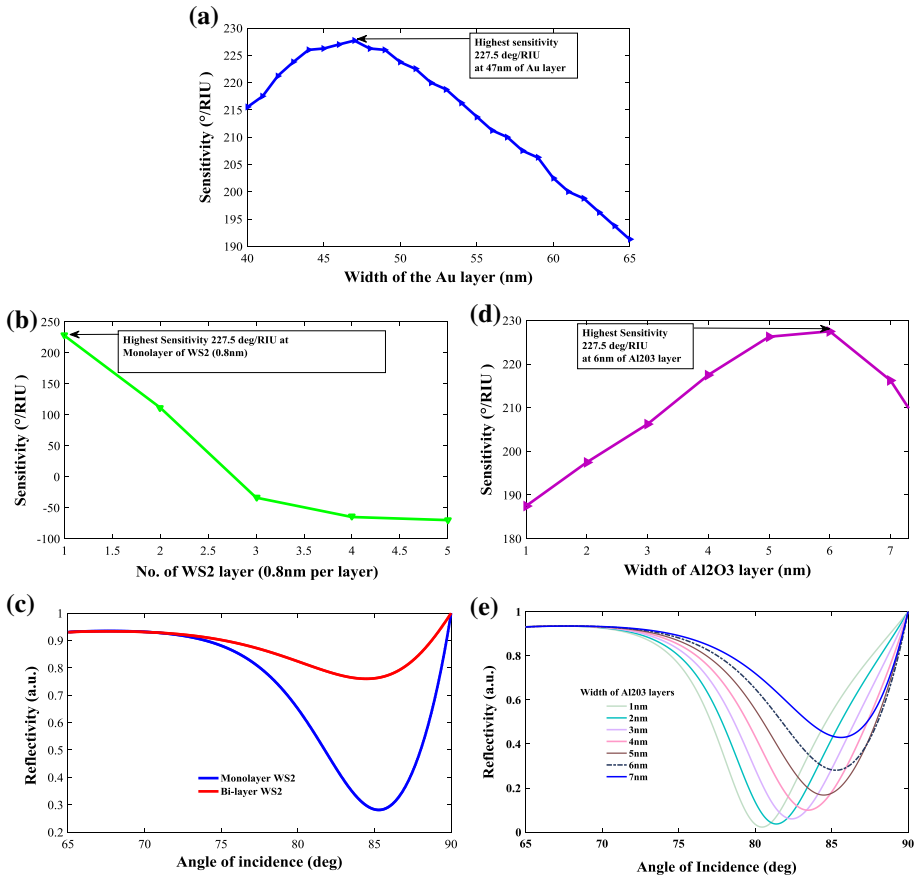
Fig. 5 **a** Sensitivity versus width of the Au layer. **b** Sensitivity versus WS$_2$ layer. **c** Reflectivity versus angle of incidence of WS$_2$. **d** Sensitivity versus Al$_2$O$_3$ layer. **e** Reflectivity versus angle of incidence of Al$_2$O$_3$

Table 2 Al$_2$O$_3$ layers are varied keeping the WS$_2$ layer absent

No. of Al$_2$O$_3$ layers	$\delta\theta$	R$_{min}$	FWHM	Sensitivity (°/RIU)	DA	Q (RIU^{-1})
1	6.4	0.000946	5.25	160	30.476	1.219
2	6.55	0.000259	5.35	163.75	30.607	1.224
3	6.8	0.00000823	5.7	170	29.824	1.1929
4	7.05	0.000643	6	176.25	29.375	1.175
5	7.3	0.0029	6.25	182.5	29.2	1.168
6	7.65	0.0079	6.55	191.25	29.198	1.1679
7	8.05	0.0181	6.8	201.25	29.595	1.1838

are shifted because of changing the number of Al$_2$O$_3$ layers. In MATLAB simulation each Al$_2$O$_3$ layer is considered as 1 nm, consequently the optimized thickness of the concerning layer is set at 6 nm.

Table 3 Al_2O_3 layers are varied keeping a monolayer of WS_2

No. of Al_2o_3 layers	$\delta\theta$	R_{min}	FWHM	Sensitivity (°/RIU)	DA	Q(RIU^{-1})
1	7.5	0.0229	7.2	187.5	26.04	1.0416
2	7.9	0.0370	7.5	197.5	26.33	1.0533
3	8.25	0.0602	7.85	206.25	26.27	1.0509
4	8.7	0.0996	8	217.5	28.26	1.0875
5	9.05	0.1682	8.1	226.25	27.93	1.1173
6	9.01	0.2809	8.05	227.50	28.26	1.1123
7	8.65	0.4295	7.95	216.25	27.2	1.088

Table 4 Sensitivity comparison of different reported prism based SPR biosensors

References	Configuration	Wavelength (nm)	Sensitivity (º/RIU)	Q (RIU^{-1})	DA
Mishra et al. (2015)	Prism/Au/Si	632	106.29	–	–
Ouyang et al. (2016)	Prism/Au/Si/MoS_2	633	131.70	–	–
Rahman et al. (2018)	Prism/Au/WS_2/Gr	633	95.71	25.19	1.763
Proposed	Prism/Au/Al_2O_3/WS_2	633	227.50	28.26	1.1123

Eventually, it is realized that by increasing the number of WS_2 layers negative invalid sensitivity can be detected which is not acceptable. That is why the number Al_2O_3 layer is varied instead of WS_2 layer. In afterwards simulation, the number of Al_2O_3 layers is varied considering two different cases. In the first case, the number of Al_2O_3 layers are varied keeping the WS_2 layer absent and the corresponding values of the parameters are listed below in Table 2. In the second case, no of the Al_2O_3 layers are varied keeping a monolayer of WS_2 and corresponding results are summarized in Table 3. Here the reason behind taking only one layer of WS_2 is that after optimizing it is found that monolayer of WS_2 gives the highest sensitivity. When two sets of values from Tables 2 and 3 are compared with each other, it is found that without WS_2 layer, seven layers of Al_2O_3 gives the highest values for sensitivity, quality factor and detection accuracy. But with a monolayer of WS_2, six layers of Al_2O_3 gives the best possible values for all three parameters.

Table 4 shows a comparison among the previous reported results and the proposed models respectively. The comparison result substantiates that among the all results, the proposed model has the highest sensitivity and quality factor.

5 Conclusion

Our proposed five-layer prism-based SPR biosensor model using Au, Al_2O_3 and WS_2 exhibits the improved sensitivity, quality factor and detection accuracy. The thickness of all layers are optimized to get the best possible result. Refractive indices of each layer for 633 nm wavelength are given as input in the MATLAB code for the simulation. Layer

optimization is mainly done on the basis of sensitivity and angular shift. Several simulations have been carried out by changing the thickness of each layer in the MATLAB code to accomplish the most satisfactory outcome. In angular modulation mode due to the optical properties of the layers used in the biosensor highest sensitivity of 227.50°/RIU is achieved. The maximum value of the other two performance parameters e.g. the quality factor and the detection accuracy are respectively 28.26 RIU^{-1} and 1.1123.

References

Albers, W.M., Vikholm-Lundin, I.: Surface plasmon resonance on nanoscale organic films. In: Carrara, S. (eds.) Nano-Bio-Sensing, pp. 83–125. Springer, New York (2011)

Biednov, M., Tatyana, L., Pavel S.: Gold and aluminum based surface plasmon resonance biosensors: sensitivity enhancement. In: Proc. SPIE 9506, Optical Sensors 2015, 95061P, 5 May 2015 (2015). https://doi.org/10.1117/12.2177992

Boisdé, G., Alan, H.: Chemical and Biochemical Sensing with Optical Fibers and Waveguides. Artech House Publishers, London (1996)

Heideman, R.G., Kooyman, R.P.H., Jan, G.: Performance of a highly sensitive optical waveguide Mach–Zehnder interferometer immunosensor. Sens. Actuators B Chem **10**(3), 209–217 (1993)

Homola, J.: Present and future of surface plasmon resonance biosensors. Anal. Bioanal. Chem. **377**(3), 528–539 (2003)

Homola, J., Marek, P.: Surface plasmon resonance (SPR) sensors. In Homola, J. (ed.) Surface Plasmon Resonance Based Sensors. Springer Series Chemical Sensors and Biosensors, vol. 4, pp. 45–67. Springer, Berlin (2006)

Kretschmann, E., Raether, H.: Radiative decay of non radiative surface plasmons excited by light. Z. für Naturforschung A **23**(12), 2135–2136 (1968)

Lin, Z., Jiang, L., Leiming, W., Guo, J., Dai, X., Xiang, Y., Fan, D.: Tuning and sensitivity enhancement of surface plasmon resonance biosensor with graphene covered Au–MoS$_2$–Au Films. IEEE Photonics J. **8**(6), 1–8 (2016)

Matsubara, K., Kawata, S., Minami, S.: A compact surface plasmon resonance sensor for measurement of water in process. Appl. Spectrosc. **42**(8), 1375–1379 (1988)

Mishra, A.K., Mishra, S.K., Verma, R.K.: An SPR-based sensor with an extremely large dynamic range of refractive index measurements in the visible region. J. Phys. D Appl. Phys. **48**(43), 435502 (2015)

Otto, A.: Excitation of nonradiative surface plasma waves in silver by the method of frustrated total reflection. Z. für Phys. A Hadrons Nucl. **216**(4), 398–410 (1968)

Ouyang, Q., Zeng, S., Jiang, L., Hong, L., Xu, G., Dinh, X.Q., Qian, J., et al.: Sensitivity enhancement of transition metal dichalcogenides/silicon nanostructure-based surface plasmon resonance biosensor. Sci. Rep. **6**, 28190 (2016)

Ouyang, Q., Zeng, S., Jiang, L., Junle, Q., Dinh, X.-Q., Qian, J., He, S., Coquet, P., Yong, K.-T.: Two-dimensional transition metal dichalcogenide enhanced phase-sensitive plasmonic biosensors: theoretical insight. J. Phys. Chem. C **121**(11), 6282–6289 (2017)

Pal, S., Verma, A., Prajapati, Y.K., Saini, J.P.: Influence of black phosphorous on performance of surface plasmon resonance biosensor. Opt. Quant. Electron. **49**(12), 403 (2017)

Pei, R., Cui, X., Yang, X., Wang, E.: Real-time immunoassay of antibody activity in serum by surface plasmon resonance biosensor. Talanta **53**(3), 481–488 (2000)

Pumera, M.: Graphene in biosensing. Mater. Today **14**(7–8), 308–315 (2011)

Rahman, M.S., Hasan, M.R., Rikta, K.A., Anower, M.S.: A novel graphene coated surface plasmon resonance biosensor with tungsten disulfide (WS 2) for sensing DNA hybridization. Opt. Mater. **75**, 567–573 (2018)

Rowe-Taitt, C.A., Hazzard, J.W., Hoffman, K.E., Cras, J.J., Golden, J.P., Ligler, F.S.: Simultaneous detection of six biohazardous agents using a planar waveguide array biosensor. Biosens. Bioelectron. **15**(11–12), 579–589 (2000)

Sharma, N.K.: Performances of different metals in optical fibre-based surface plasmon resonance sensor. Pramana **78**(3), 417–427 (2012)

Shushama, K.N., Rana, M.M., Inum, R., Hossain, M.B.: Graphene coated fiber optic surface plasmon resonance biosensor for the DNA hybridization detection: simulation analysis. Opt. Commun. **383**, 186–190 (2017a)

Shushama, K.N., Rana, M.M., Inum, R., Hossain, M.B.: Sensitivity enhancement of graphene coated surface plasmon resonance biosensor. Opt. Quant. Electron. **11**, 381 (2017b)

Stewart, M.E., Anderton, C.R., Thompson, L.B., Maria, J., Gray, S.K., Rogers, J.A., Nuzzo, R.G.: Nanostructured plasmonic sensors. Chem. Rev. **108**(2), 494–521 (2008)

Tumolo, T., Angnes, L., Baptista, M.S.: Determination of the refractive index increment (dn/dc) of molecule and macromolecule solutions by surface plasmon resonance. Anal. Biochem. **333**(2), 273–279 (2004)

Verma, A., Prakash, A., Tripathi, R.: Sensitivity enhancement of surface plasmon resonance biosensor using graphene and air gap. Optics Communications **357**, 106–112 (2015)

Wang, G., Arwin, H., Jansson, R.: An optical gas sensor based on ellipsometric readout. IEEE Sens. J. **3**(6), 739–743 (2003)

Wolfbeis, O.S.: Fiber Optic Chemical Sensors and Biosensors, vol. 1. CRC, Boca Raton (1991)

Wu, L., Chu, H.S., Koh, W.S., Li, E.P.: Highly sensitive graphene biosensors based on surface plasmon resonance. Opt. Express **18**(14), 14395–14400 (2010)

Zeng, S., Siyi, H., Xia, J., Anderson, T., Dinh, X.-Q., Meng, X.-M., Coquet, P., Yong, K.-T.: Graphene–MoS2 hybrid nanostructures enhanced surface plasmon resonance biosensors. Sens. Actuators B: Chem. **207**, 801–810 (2015)

Zhao, J., Xiaoyu, Z., Chanda, R. Y., Amanda, J. H., Van Duyne, R. P. (eds.) Localized surface plasmon resonance biosensors, pp. 219–228 (2006)